13th IEA Heat Pump Conference
April 26-29, 2021 Jeju, Korea

A novel geothermal heat pump system integrated with underground thermal storage for shifting building electric demands

Liang Shi[a], Ming Qu[a], Xiaobing Liu[b*]

[a]Purdue University, School of Civil Engineering, West Lafayette, IN 47906, USA
[b]Oak Ridge National Laboratory, Oak Ridge, TN 37831, USA

Abstract

The intermittent supply of renewable power and the continuous increase of electric demands pose challenges to the stability of existing electric grids and utilization efficiency of renewable power. The thermal energy storage applied to buildings is capable of utilizing the overproduced renewable power to store thermal energy, which is later discharged to meet thermal demands of buildings when renewable power production decreases. A novel geothermal heat pump system incorporated with underground thermal energy storage was investigated through a case study of applying the proposed system to a residential building in Baltimore, Maryland. A transient one-dimensional heat transfer model of the proposed dual-purpose underground thermal battery (DPUTB) was developed and integrated with simulation models of a dual source heat pump (DSHP) and a typical residential building to form a quasi-steady-state model of the proposed system. Simulation results indicate that the proposed system can shift the building electric demand from peak hours to other times when electricity is cheap. In a cooling season, the electricity consumption during peak hours is reduced by 40% and the associated electricity cost is reduced by 20%.

Selection and/or peer-review under responsibility of the organizers of the 13th IEA Heat Pump Conference 2020.

Keywords: underground thermal energy storage; geothermal heat pump; electric load shifting

1. Introduction

In the U.S., the penetration of renewable power generation has increased to reduce greenhouse gas emissions. However, the intermittent outputs of renewable energy pose challenges to the existing electric grid. The grid operators curtail renewable power when the power production is greater than the demand from the consumer. Thus, it reduces the economic and environmental benefits of renewable power [1]. When renewable energy is not available (sunsets, cloudy, etc.), the power demand from the existing grid increases dramatically. It requires the electricity generators ramp up their production rate quickly, resulting in low operating efficiency and high power production cost.

Buildings consume 73% of all U.S. electricity according to Energy Information Administrator [2]. The electricity consumed for space heating and cooling counts 22% and 14% of the total electricity consumption in residential and commercial buildings, respectively, on an annual basis [3]. It means that space heating and cooling for buildings is responsible for 13% of the total electricity consumption each year in the U.S.

Thermal energy storage (TES) is a promising technology that allows storing heat (or cooling energy) generated with overproduced renewable power, or electricity from the grid during off-peak hours, and using them to meet the thermal demands of buildings during peak hours. One promising technology is the integration of TES with heat pump systems [4]. Heat pump technologies utilize electricity to provide space cooling and/or space heating, as well as domestic water heating. The TES integrated heat pump systems provide valuable load

* Corresponding author. Tel.: +1-865-574-2593
E-mail address: liux2@ornl.gov

shifting resources to utility companies for reducing its operation cost while meeting the demands for electricity, without increasing power generation capacity [5].

TES can be integrated into a building's thermal system in passive or active ways. The passive applications usually utilize the existing thermal mass of the building. However, it is difficult to control the charging and discharging rate in passive applications, and normally more energy is consumed due to high thermal loss to the ambient. On the other hand, the active applications utilize a dedicated TES and associated heating/cooling system to charge and discharge the TES with more precise control.

Stratified water tanks are widely used for demand side management (DSM) due to its availability and low cost [5-7]. Stratified water tanks integrated with air source heat pump (ASHP) for heating application in residential buildings are investigated before. Renaldi et al. [6] proposed an optimization method to minimize the total operating cost of the system. The simulation result indicated that 6% energy cost reduction can be achieved with the proposed system compared with a conventional gas boiler system when a time-of-use electricity rate is available. Arteconi et al. [5] applied a DSM strategy to shift electric load during 3-hour peak hours to off-peak hours. They concluded that by adding a water tank to the heat pump system, the load shifting effect can be realized without influencing the indoor thermal comfort. However, 4% more electricity was consumed compared to the baseline heat pump system (without TES). Stratified water tanks are also applied for DSM in cooling applications. Yan et al. [7] proposed an active TES using chilled water tank in an office building in Hong Kong. The simulation results showed that the proposed system was able to reduce the capacity of the chiller by 24%. However, 2.6% more electricity was consumed due to additional pumping and thermal loss from the TES tank.

Besides water tanks, phase change material (PCM) tanks [8,9] are also applied to heat pump systems for DSM because of the high energy storage density of PCMs during phase change process. Most previous studies for PCM tank integrated thermal systems are for heating application only. Lizana et al. [8] integrated a stratified PCM tank with an air-water heat pump (AWHP) in a residential building in UK and proposed a DSM strategy to minimize the electric cost by utilizing a time-of-use (TOU) electric rate tariff. The simulation results indicate a 20% electricity cost reduction, while the total electricity consumption increased by 8%. Hirmiz et al. [9] customized a hybrid PCM water tank and integrated it with a ground source heat pump (GSHP) in a residential building in Canada. The system could shift the peak electric demand during 6-hour to off-peak hours. In addition, by applying PCM, the tank volume was reduced by 3 folds compared with using water tanks.

Previous studies concluded that TES integrated heat pump systems could make the electric demand of a building more flexible. With appropriate sizing, the system can shift electric demand from peak period (3 to 6 hours) to off-peak period. If time-of-use electricity rate is available, the load shifting can lead to significant (up to 20%) electricity cost savings. In addition, by applying TES, capacity of the heat pump can be smaller. However, the TES integrated systems always consume more energy (3% - 8% increase) than conventional systems due to the heat loss from the TES tank and the additional pumping power. Moreover, most studies used ASHPs due to their low cost and easy installation. However, the efficiency of an ASHP is usually lower than a GSHP, especially in cold climates. TES tanks in previous studies are installed above the ground, which not only occupy floor area, but also be heavily insulated to reduce heat loss. Besides, neglected by most previous studies, the cost of the TES integrated system is high due to additional component for TES. As a result, its applications is limited despite of its potential benefits to both the building owners and the grid operators.

The current study proposes a novel geothermal heat pump system integrated with an underground thermal energy storage to make the electricity demand of buildings flexible. The proposed system includes a state-of-art design for a dual-purpose underground thermal battery (DPUTB), which combines TES and ground heat exchanger (GHE) into one tank to reduce the initial cost and does not occupy any floor space and roof area for installation. A dual-source heat pump (DSHP) as the second main component of the proposed system can not only achieve higher efficiency than ASHPs, but also reduce the needed size of GHEs. Because the DPUTB is installed underground and any heat loss from the TES can be recovered though the GSHP operation, there is little heat loss to the ambient. This paper presents a preliminary study of the load shifting capability, thermal performance, and associated operating costs of the proposed system.

2. System Description

The proposed system consists of a DSHP and a DPUTB as depicted in Fig. 1. The DSHP is an electricity-driven heat pump using vapor compression refrigeration cycle, which utilizes either the ambient air or the ground as its heat source/sink. A refrigerant-to-air heat exchanger is used in the source side of the DSHP when

the ambient temperature is suitable for achieving a relatively high COP of the heat pump. When the ambient air temperature is too high in summer (or too low in winter) to be used as a heat source/sink, the heat pump switches to utilize the DPUTB as its heat source/sink (through a refrigerant-to-water heat exchanger) for a better COP. The DSHP can reduce the seasonal imbalance of the thermal loads of the GHE and thus reduce the needed size of the GHE.

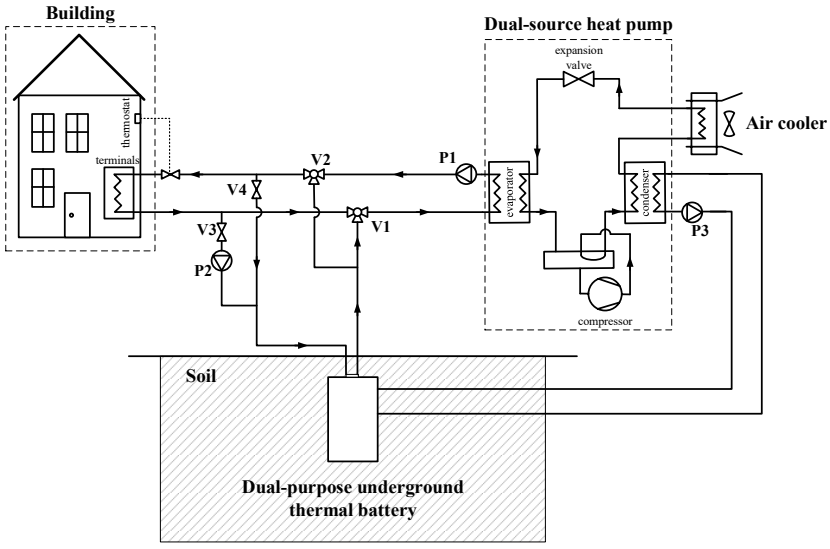

Fig. 1. System configuration diagram (cooling mode, DPUTB charging)

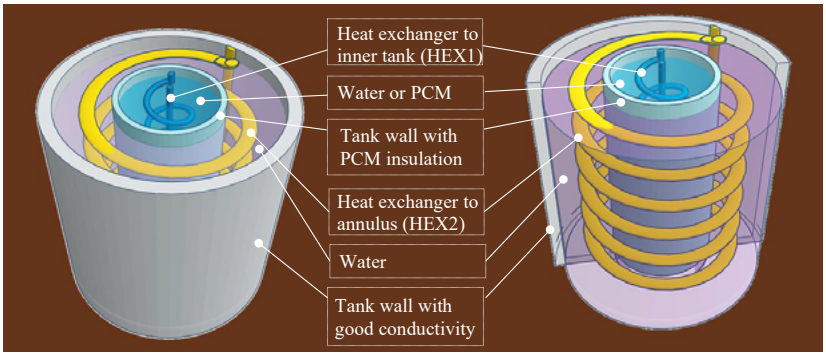

Fig. 2. Schematic of the DPUTB

The schematic of the DPUTB is shown in Fig. 2, it consists of an enclosed inner tank within a larger water tank. The inner tank works as a TES while the outer tank works as a GHE. A low-cost PCM encapsulated in a thin plastic panel is wrapped around the outer surface of the inner tank. Due to the low thermal conductivity and high latent heat of the PCM, it reduces the heat exchange between the inner and outer tanks. Another type of PCM with a different melting temperature is supplied in the inner tank for storing the thermal energy. Two coil heat exchangers are installed in the inner and outer tanks, respectively, to exchange heat with the HVAC system of the building. This design allows for storing thermal energy in the inner tank and later for providing direct heating or cooling to eliminate or reduce the electricity consumption for space heating or space cooling during peak hours of the electric grid. The outer tank of the DPUTB not only exchanges heat with the surrounding soil but also recovers energy losses from the inner tank for more efficient heat pump operation.

3. Component Modeling

3.1. DSHP

The DSHP is modelled as a combination of two conventional heat pumps: an air-water heat pump (AWHP) for air source and a water-water heat pump (WWHP) for ground source. The curve fitting models for the AWHP and the WWHP are developed based on the heat pump models (type 927 and type 941) of TRNSYS [10]. These heat pump models use performance curves of typical AWHP and WWHP units to predict their heating and cooling outputs and associated power consumption based on the inlet conditions from the condenser and evaporator. The rated COPs for AWHP and WWHP are 4.0 and 5.0, respectively.

3.2. DPUTB

A simplified one-dimensional transient model of the DPUTB has been developed in MATLAB [11] based on following assumptions and simplifications:

1. The PCM in the inner tank and the water at the outer tank are both well mixed. They are individual bulks with homogeneous properties within their domains.
2. The DPUTB is cylindrical symmetric and heat transfer occurs only along the radial direction.
3. The convection heat transfer within PCMs is neglected; only the conduction heat transfer is modeled.
4. The PCM's freezing point is identical to its melting point.

The model accounts for the following heat transfer phenomena:

1. Heat transfer between the heat exchanger in the inner tank (HEX1) and the inner tank PCM
2. Heat transfer between the heat exchanger in the outer tank (HEX2) and the outer tank water
3. Heat transfer between the inner tank PCM/water and the outer tank water through the inner tank wall and the PCM wrapped around the inner tank
4. Heat transfer between the DPUTB shell and the surrounding soil
5. Phase change process within the wrapping PCM and the inner tank PCM

3.2.1 Heat Exchanger

HEX1 and HEX2 are heat exchangers that direct contact with the inner and outer tank fluids. The input thermal energy to the tank fluid can be determined using equation (1):

$$q = UA \cdot \Delta T_{lm}, \tag{1}$$

where UA is the product of the overall heat transfer coefficient and the heat transfer area of a heat exchanger; ΔT_{lm} is the logarithm mean temperature difference between the fluid in the heat exchanger and the fluid in the tank at a given time step, which is expressed with equation (2):

$$\Delta T_{lm} = \frac{(T_{HEX,in} - T_{tank}) - (T_{HEX,out} - T_{tank})}{\ln \frac{T_{HEX,in} - T_{tank}}{T_{HEX,out} - T_{tank}}}, \tag{2}$$

where $T_{HEX,in}$ and $T_{HEX,out}$ are the heat transfer fluid temperatures at the inlet and outlet of the heat exchanger, respectively; T_{tank} is the average tank water temperature.

For the current case, the UA value of the heat exchanger is proportional to the mass flow rate of the heat exchange fluid, and it can be determined through experimental data regression.

At steady state, the heat exchange rate is also equal to the enthalpy change of the fluid in the heat exchanger, which can be determined using Eq. (3):

$$q = \dot{m}_{HEX} \cdot c_p \cdot \left(T_{HEX,in} - T_{HEX,out}\right), \tag{3}$$

where $\dot{m}_{HEX}$ is the mass flow rate of the heat transfer fluid; c_p is the specific heat of the heat transfer fluid.

The above equations are solved to determine the heat exchanger outlet temperature at a given time step with known inlet fluid temperature, thus the heat transfer rate can be calculated. The heat transfer rates from HEX1 and HEX2 are used as boundary conditions of the DPUTB model.

3.2.2 Natural convection

The empirical correlations describe the convection heat transfer coefficient between the tank fluid and its surrounding solid surfaces. The Rayleigh number and the Nusselt number can be determined using equation (4) and (5), respectively:

$$\mathrm{Ra} = \frac{g \cdot \beta \cdot |T_s - T_\infty| \cdot L^3}{\nu \cdot \alpha}, \tag{4}$$

where g is the gravitation; β is the thermal expansion coefficient; T_s is the temperature at the surface; T_∞ is the temperature of the fluid at bulk; L is the characteristic length; ν is the kinematic viscosity; and α is the thermal diffusivity.

$$\mathrm{Nu} = \left\{ 0.825 + \frac{0.387 \cdot \mathrm{Ra}^{\frac{1}{6}}}{\left[1 + (0.492/Pr)^{\frac{9}{16}}\right]^{\frac{8}{27}}} \right\}^2, \tag{5}$$

where Pr is the Prandtl number.

Thus the convective heat transfer coefficient can be determined using equation (6):

$$h_{conv} = \mathrm{Nu} \cdot \frac{k}{L}, \tag{6}$$

where k is the thermal conductivity of the fluid in the tank.

The surface temperature of the solid wall in contact with the liquid can be calculated based on the energy balance at the surface:

$$h_{conv} \cdot (T_\infty - T_s) = \frac{k_{wall}}{\Delta x} \cdot (T_s - T_{wall}), \tag{7}$$

where k_{wall} is the thermal conductivity of the solid wall; Δx is the thickness of the wall; T_{wall} is the surface temperature at the other side of the wall.

Equations (4) to (7) are solved to determine the convection heat transfer at the solid surface at a given time step.

3.2.3 Conduction heat transfer

Heat conduction is considered in the tank wall, the surrounding soil, and the wrapping PCM. For 1D heat conduction in the cylindrical coordinate, the conduction heat transfer equation can be expressed as:

$$\frac{1}{r}\frac{\partial}{\partial r}\left(r \cdot k \frac{\partial T}{\partial r}\right) = \rho \cdot c_p \frac{\partial T}{\partial t}, \tag{8}$$

where r is the position in the radial direction; ρ is the density; t is the time step.

Due to the complexity of the whole simulation domain, the explicit method is applied for the numerical calculation. Therefore, the conduction heat transfer equation is discretized into the form expressed in equation (9), subscript i represents the position along the radial direction:

$$\frac{1}{r_i} \cdot \frac{r_{i+\frac{1}{2}} \cdot k_{i+\frac{1}{2}} \frac{T_{i+1} - T_i}{\Delta r} - r_{i-\frac{1}{2}} \cdot k_{i-\frac{1}{2}} \frac{T_i - T_{i-1}}{\Delta r}}{\Delta r} = \rho \cdot c_p \frac{T_i^{new} - T_i}{\Delta t}, \tag{9}$$

The temperatures in the tank wall, the surrounding soil, and the wrapping PCM are determined at each time step with the above numerical method and given boundary conditions at each simulation domain.

3.2.4 Phase change

The latent heat accumulation method [12] is applied to simulate the phase change process within the wrapping PCM and the inner tank PCM. For a certain amount of PCM, the maximum latent heat it can store/release can be determined as:

$$Q_{latent,max} = m \cdot \Delta H, \tag{10}$$

where m is the mass of the PCM; ΔH is the specific latent heat of the PCM.

It is assumed in this model that the temperature of a PCM is kept intact when it is undergoing phase change process. The phase change process is indicated with a 'solid fraction' factor. The 'solid fraction' factor during the melting process of a PCM is quantified using following equation:

$$\theta = 1 - \frac{Q_{latent,acc}}{Q_{latent,max}}, \tag{11}$$

where $Q_{latent,acc}$ is the accumulated latent heat in the PCM during phase change; $Q_{latent,max}$ is the maximum latent heat the PCM can store.

In this model, the PCM wrapping around the inner tank is modeled as a series of coaxial hollow cylinders and each hollow cylinder has uniform temperature and phase status. The temperature and phase status of each hollow cylinder is updated at the end of each time step after calculating the heat transfer within the PCM domain. The inner tank PCM is modeled as one volume with uniform temperature and phase status, which is updated at each time step based on the heat transferred from the heat exchanger and through the wall of the inner tank.

3.3. Control Strategy

The integrated DSHP and DPUTB system can be operated in ten different modes, as listed in table 1. To achieve specific goals (e.g., energy cost reduction, load leveling, etc.), different control strategies can be developed to determine the operation mode at a given time of a day. In this study, a rule-based control strategy is developed to shift the electric demand of the building from peak hours to off-peak hours so that it can take advantage of the time-of-use (TOU) electric tariff to reduce the energy cost of the building. The logic flow chart of this control strategy is shown in Fig. 3.

Table 1. System operation mode description

Mode #	Building Load	Heat Pump Status	TES Status
1	no	off	off
2	yes	off	discharge
3	yes	air-source	off
4	yes	ground-source	off
5	yes	air-source	charge
6	yes	ground-source	charge
7	yes	air-source	discharge
8	yes	ground-source	discharge
9	no	air-source	charge
10	no	ground-source	charge

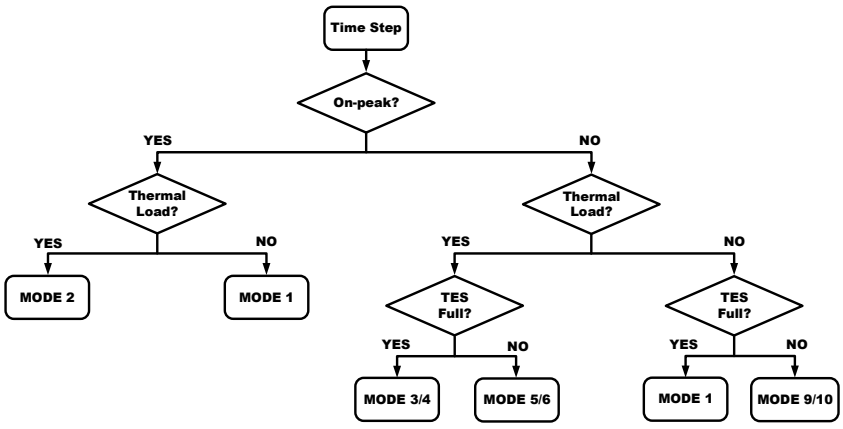

Fig. 3. Control strategy for reducing energy cost

4. Case Study

4.1. Building Information and Equipment Sizing

A typical U.S. residential building [13] in Baltimore, Maryland is chosen for a case study. It is a single-family detached house located with 223 m^2 air-conditioned floor space. The air-conditioning system is a centralized constant volume air system with on/off control to maintain the room temperature within 22.2 to 23.9 °C. The nominal cooling capacity of the air-conditioner used in the building is 2-ton (7 kW) and its nominal COP is 3.97. This air-conditioner is used as a baseline in this study to be compared against the integrated DSHP and DPUTB system.

A pilot TOU electric tariff is used in this study. This TOU electric tariff named 'Schedule RD' was introduced by the Baltimore Gas and Electricity Company for residential customers who have installed smart meters. According to this tariff, during the summer of 2019, the electricity retail price is 0.339 $/kWh between 14:00 and 19:00 on weekdays, which is defined as on-peak hours, and it is 0.064 $/kWh during other time (off-peak hours) [14].

The sizes of the DSHP and the DPUTB are determined based on the thermal load of the building and the control strategy described in Section 3.3. The thermal energy storage capacity of the DPUTB should be no less than the total thermal load during on-peak hours of the design day. It ensures that the stored thermal energy is adequate for providing space cooling during the on-peak period, and thus the heat pump can be turned off to reduce electric demand. The capacity of the heat pump could be smaller than the peak cooling load of the building during a cooling season, but it should be larger than the maximum cooling load during the off-peak period so that it can simultaneously cools the inner tank for storing sufficient cooling energy while providing space cooling during the off-peak hours. To meet the cooling load of the residential building, two identical DPUTBs are needed, and the nominal cooling capacity of the DSHP is 1.75-ton (6.125 kW), which is 12.5% smaller than the baseline air-conditioner. The key parameters of the DPUTB are listed in table 2.

Table 2. Key parameters of the system components

Property	Value	Unit
DPUTB dimensions		
Inner tank diameter	39	cm
Inner PVC shell thickness	0.55	cm
PCM blanket thickness	2.54	cm
Outer tank diameter	101.37	cm
Outer PVC shell thickness	0.82	cm
Height of the inner tank	609.60	cm
Height of the outer tank	609.60	cm
Inner shell thermo-physical properties		
Material	PVC	–
Thermal conductivity	0.19	W/m K
Density	1380	kg/m^3
Specific heat	1000	J/kg K
Outer shell thermo-physical properties		
Material	HDPE	–
Thermal conductivity	0.50	W/m K
Density	950	kg/m^3
Specific heat	1900	J/kg K
Inner tank PCM thermo-physical properties		
Melting point	13	°C
Heat of fusion	160	kJ/kg
Density (solid)	917.5	kg/m^3
Density (liquid)	998	kg/m^3
Thermal conductivity (solid)	2.25	W/m K
Thermal conductivity (liquid)	0.6	W/m K
Specific heat (solid)	2027	J/kg K
Specific heat (liquid)	4182	J/kg K

Annulus PCM thermo-physical properties		
Melting point	15	°C
Heat of fusion	160	kJ/kg
Density	1118	kg/m^3
Thermal conductivity (solid)	0.1489	W/m K
Thermal conductivity (liquid)	0.1596	W/m K
Specific heat (solid)	3000	J/kg K
Specific heat (liquid)	2740	J/kg K
Soil thermos-physical properties		
Thermal conductivity	1.70	W/m K
Density	1602	kg/m^3
Specific heat	2100	J/kg K
Undisturbed ground temperature	14.4	°C
Heat exchanger properties		
UA value	5000	W/°C

4.2. System Simulation

Numerical models of DPUTB and DSHP, as well as the control strategy, are implemented in MATLAB and integrated together to simulate the performance of the integrated DPUTB and DSHP system at each time step (60 seconds).

The hourly cooling load and electricity consumption of the building resulting from using the baseline air-conditioner during the entire cooling season is obtained from computer simulation of the residential building using typical meteorological year (TMY3) weather data [15]. The simulation-predicted hourly cooling load is used as the inputs to the simulation model of the integrated DPUTB and DSHP system.

4.3. Design-Day Simulation Results

Some featured results for a design-day (July 21) simulation of the integrated DPUTB and DSHP system with the rule-based control strategy are shown in Fig. 4. The first sub-figure clearly shows that a considerable amount of electricity demand has been shifted from on-peak (14:00 – 19:00) to off-peak hours.

From 0:00 to 8:00, due to the relatively low ambient temperature, the DSHP operates as an ASHP to supply space cooling to the building as well as to charge the DPUTB. The operating COP of the ASHP is stabilized at around 5 (4th subplot). The solid fraction of the inner tank PCM keeps increasing until it is fully charged (i.e., when the average temperature of the PCM is 3ºC lower than its melting temperature) at around 6:00 (3rd subplot). As long as the inner tank is fully charged, the heat pump solely operates to satisfy the cooling demand of the building. Otherwise, the heat pump works to charge the inner tank and to meet the thermal load of the building simultaneously. During this period, there is no heat rejection to the outer tank of the DPUTB. Thus, the temperature of the outer tank water is slightly cooled down by the inner tank and the surrounding soil, as can be observed from the 2nd subplot.

From 8:00 to 14:00, while it is still in the off-peak period, the ambient temperature is higher than 26.7 ºC, which is the threshold for switching from ASHP to GSHP. Therefore, instead of rejecting condensing heat to the ambient air via the refrigerant-to-air heat exchanger, the DSHP rejects condensing heat to the soil via the heat exchanger in the outer tank of the DPUTB. It can be observed from the 2nd subplot that the outer tank water temperature increases and the heat transfer rate from the tank to the soil also increases (5th subplot). The average operating COP of the GSHP is around 5.5 (4th subplot), and it decreases with the increase of the outer tank temperature.

The on-peak period begins at 14:00 and ends at 19:00. During this period, the heat pump is completely turned off (5th subplot), and the cooling energy stored in the inner tank of the DPUTB is used to meet the thermal load of the building. A significant reduction of the stored cooling energy can be observed from the decreasing trend of the solid factor of the PCM as shown in the 3rd subplot. Since the heat pump is turned off, there is no heat rejected to the outer tank of the DPUTB, and its temperature is cooled down by the surrounding soil, as depicted in the 2nd subplots. After 19:00 (the end of the peak hours), the heat pump is turned on to simultaneously cool the building and the inner tank of the DPUTB. It can be observed that right after 19:00, the electric demand of the integrated DPUTB and DSHP system is higher than the baseline, this is because that

the DSHP operates at its full capacity to meet the building thermal load and to charge the DPUTB at the same time, while for the baseline case, the air conditioner only works partially to meet the building thermal demand.

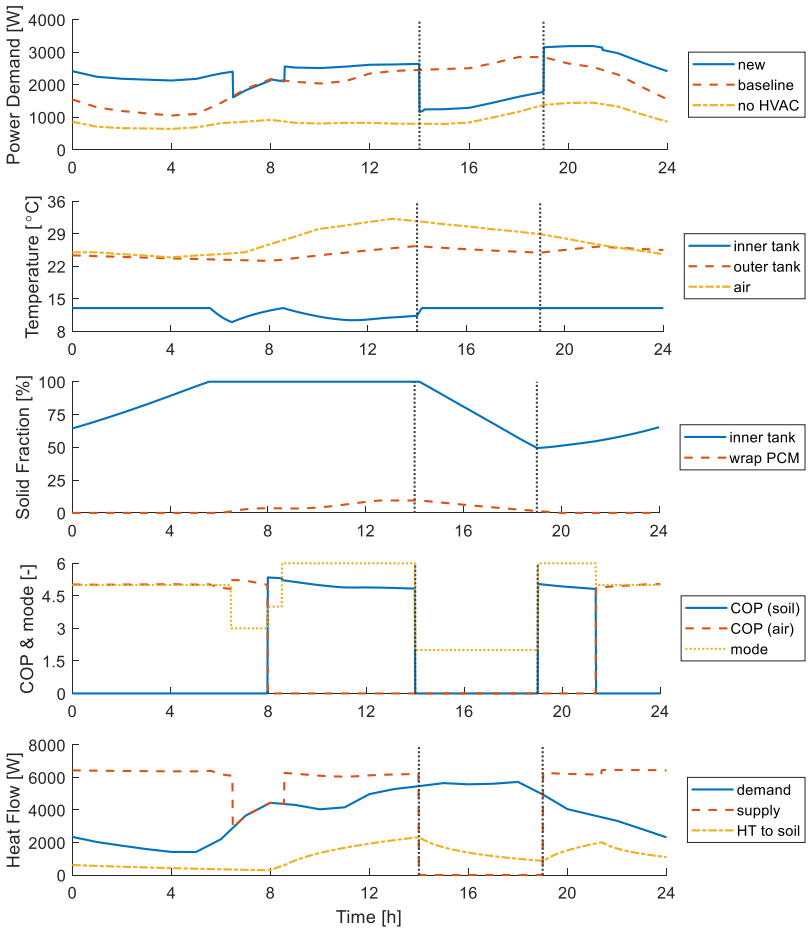

Fig. 4. Featured simulation results of the integrated DPUTB and DSHP system on the design-day (July 21)

The power consumption and the electricity cost of the design day are summarized in Table 3. The result shows that by applying the novel system with the rule-based control strategy, the daily electricity consumption is increased by 11%. However, the on-peak electricity consumption contribution (on-peak electricity consumption divided by total daily electricity consumption) is reduced from 26.9% to 13.1%. The electricity cost is reduced by 19.5%. It indicates that the novel system with the proposed control strategy can effectively shift the electric load from on-peak to off-peak period, but more electricity is consumed during the whole day.

Table 3. Energy consumption and cost for design-day simulation with rule-based control

System	Control	Total electricity consumption [kWh]	On-peak electricity consumption [kWh]	Cost [$]
Baseline	conventional on/off	49.06	13.21	6.77
Novel	rule-based control	54.43	7.14	5.45

4.4. Simulation Results of a Cooling Season

A seasonal simulation (June 1 to September 30) is conducted to investigate the long-term performance of the integrated DPUTB and DSHP system. Fig. 5 shows some of the simulation results. The 1st subplot of Fig. 5 indicates that, with the cost-reduction oriented control strategy, the hourly electric demand of the integrated DPUTB and DSHP system fluctuates within 640 – 3500W in each day. Overall, this control strategy cannot flatten the electric demand profile of the building. To achieve load leveling with the integrated system, a different control strategy needs to be used. During the entire cooling season simulation, the outer tank water temperature ranges from 15 ºC to 30 ºC (2nd subplot), which ensures the DSHP operate at a relatively high COP when it switches to ground source. The air source operation of the DSHP (when the ambient temperature is relatively low) gives more time to the outer tank for dissipating heat to the surrounding soil and thus cools down the outer tank water temperature. As shown in the 2nd subplot, the outer tank water temperature recovers to its original level after the entire cooling season operation. The 3rd subplot shows the solid fraction profile of the inner tank PCM and wrapping PCM. The stored latent cooling energy of the inner tank PCM never exhausted, which indicates that the sizing of the DPUTB is reasonable. The wrapping PCM is solid at the beginning of the cooling season because its melting temperature (15 °C) is higher than the surrounding soil temperature (14.4 °C). The wrapping PCM is melted gradually after cooling season starts, as indicated by the decrease of its solid fraction. The wrapping PCM cycles between melting and solidification on a daily basis (i.e., melting when heat from the GSHP is rejected into the outer tank, and re-solidifying when releasing heat to the surrounding soil and the inner tank). The simulation result indicates that the DPUTB maintains a significant temperature difference between the inner and outer tank every day.

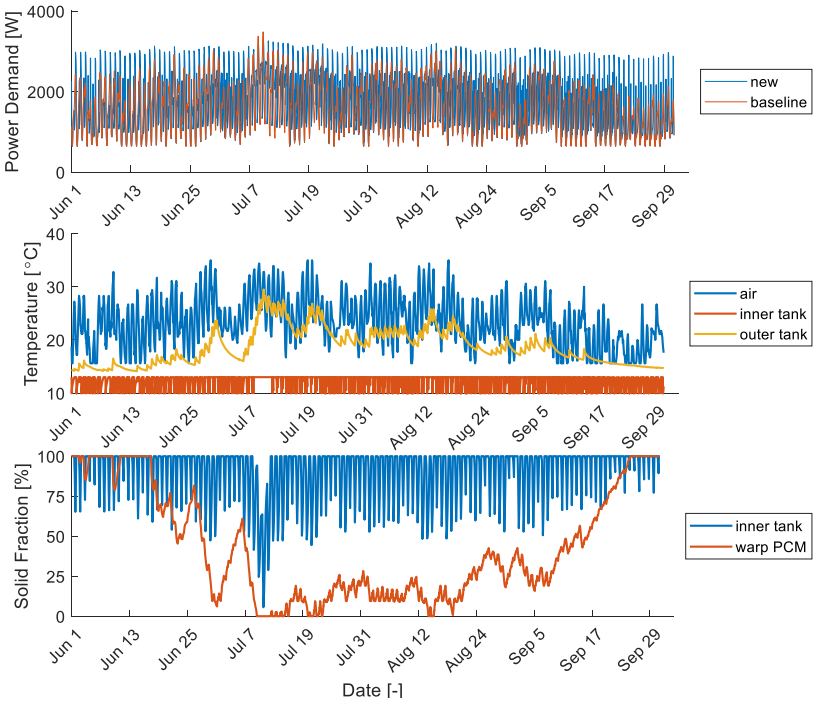

Fig. 5. Featured simulation results of the integrated DPUTB and DSHP system during a cooling season

The electricity consumption and the associated cost during the entire cooling season are listed in Table 4. These data show that although the electricity consumption of the entire building (including both HVAC and non-HVAC electric consumption) is increased by 4.5%, the on-peak electricity consumption of the building is

reduced by 40% compared with that resulting from using the baseline air-conditioner, and the electricity cost is reduced by 19.5% over the entire cooling season.

Table 4. Energy consumption and cost for seasonal simulation with rule-based control

System	Control	Total electricity consumption [kWh]	On-peak electricity consumption [kWh]	Cost [$]
Baseline	conventional on/off	4764	1333	671
Novel	rule-based control	4978	805	540

5. Conclusions

This study conducts a preliminary evaluation of a novel dual-source heat pump (DSHP) integrated with an underground thermal energy storage system (DPUTB) for shifting the electric demand of a residential building in the United States during a cooling season. A simplified numerical model has been developed for the DPUTB. A computer simulation of the integrated DPUTB and DSHP system is conduced to evaluate its load shifting performance and resulting energy cost. Following conclusions can be drawn from the simulation results:

- The system shifts 5-hour on-peak electricity consumption for space cooling to off-peak period, which results in a 40% reduction in the peak electricity consumption of the building over the entire cooling season
- The associated electricity cost reduction is around 20%, which is higher than other active TES systems reported in existing literature
- The heat pump capacity is reduced by 12.5% compared with the baseline air-conditioner, which does not have any TES
- The COP of the DSHP remains high (around 5) during the cooling season
- Total electricity consumption increases by 4.5% over the cooling season due to additional pumping

Further work includes optimizing the charging control of the inner tank and applying better thermal insulation to reduce heat transfer between the inner tank and the outer tank. It is also planned to investigate the heating season performance of the integrated system. More advanced controls, such as model-based control or artificial intelligence, will also be investigated for improving the capability of the integrated system for effectively reshape the electric demand profile in response to the demand side management signal of the electric grid while satisfying all the thermal demands of the building.

Acknowledgements

The authors thank the Low-Temperature Geothermal Program of the Geothermal Technologies Office at the U.S. Department of Energy for funding this research project.

References

[1] NREL (2015). Overgeneration from Solar Energy in California: A Field Guide to the Duck Chart. https://www.nrel.gov/docs/fy16osti/65023.pdf.
[2] EIA (2019), Electric Power Monthly with Data for August 2019. https://www.eia.gov/electricity/monthly/current_month/epm.pdf.
[3] Schwartz, L. et al. (2017). Electricity end uses, energy efficiency, and distributed energy resources baseline.
[4] Lizana, J., Chacartegui, R., Barrios-Padura, A., & Ortiz, C. (2018). Advanced low-carbon energy measures based on thermal energy storage in buildings: A review. *Renewable and Sustainable Energy Reviews*, *82*, 3705-3749.
[5] Arteconi, A., Hewitt, N. J., & Polonara, F. (2013). Domestic demand-side management (DSM): Role of heat pumps and thermal energy storage (TES) systems. *Applied thermal engineering*, *51*(1-2), 155-165.
[6] Renaldi, R., Kiprakis, A., & Friedrich, D. (2017). An optimisation framework for thermal energy storage integration in a residential heat pump heating system. *Applied energy*, *186*, 520-529.
[7] Yan, C., Xue, X., Wang, S., & Cui, B. (2015). A novel air-conditioning system for proactive power demand response to smart grid. *Energy conversion and management*, *102*, 239-246.

[8] Lizana, J., Friedrich, D., Renaldi, R., & Chacartegui, R. (2018). Energy flexible building through smart demand-side management and latent heat storage. *Applied energy*, *230*, 471-485.
[9] Hirmiz, R., Teamah, H. M., Lightstone, M. F., & Cotton, J. S. (2019). Performance of heat pump integrated phase change material thermal storage for electric load shifting in building demand side management. *Energy and Buildings*, *190*, 103-118.
[10] Klein, S. A. et al. (2017). "TRNSYS 18: A Transient System Simulation Program." Solar Energy Laboratory, University of Wisconsin, Madison. http://sel.me.wisc.edu/trnsys.
[11] MATLAB version 9.4 (2018). Natick, Massachusetts: The MathWorks Inc.
[12] Muhieddine, M., Canot, E., and March, R. (2009). Various approaches for solving problems in heat conduction with phase change. *International Journal on Finite Volumes*, 19.
[13] DOE, Residential Prototype Building Models. https://www.energycodes.gov/development/residential/iecc_models
[14] Baltimore Gas and Electricity Company (2018). Residential delivery and energy time-of-use pilot – electric schedule RD. https://www.bge.com/MyAccount/MyBillUsage/Documents/Electric/Schedule_RD.pdf
[15] Wilcox, S. and W. Marion. (2008). User's Manual for TMY3 Data Sets, NREL/TP-581-43156. April 2008. Golden, Colorado: National Renewable Energy Laboratory.